Research Article

Hangyu Zhu*, Lanqing Wang, Jianli Li*, Jixuan Zhao, and Yue Yu

Effects of metallurgical factors on reticular crack formations in Nb-bearing pipeline steel

https://doi.org/10.1515/htmp-2020-0043
Received Oct 26, 2019; accepted Feb 09, 2020

Abstract: Microscopic morphologies of reticular cracks in Nb-bearing pipeline surfaces are shown in this work. A decarburization layer, oxidized round spots, and the distributions of residual elements are each detected to better understand the mechanisms of reticular crack formations. The results show that reticular cracks are discontinuously distributed and filled with iron oxide. The oxidized round spots near the crack sides are larger and more intensive than steel matrix, with primary chemical compositions of Fe, Mn, and Si oxides. There is no obvious enrichment of Cu, Cr, or Sn near the crack zones. The formation of reticular cracks occurs prior to both decarburization and the formation of oxidized round spots. The ferrite potential (FP) of the examined pipeline steel is 1.05, which leads to a higher relative crack susceptibility. It is concluded that reticular cracks are generated during the continuous casting solidification process due to the extension of intergranular microcracks along grain boundaries under the abnormal conditions of the continuous casting process.

Keywords: surface defect; reticular crack; pipeline steel; oxidized round spots

***Corresponding Author: Hangyu Zhu:** The State Key Laboratory of Refractories and Metallurgy, Wuhan University of Science and Technology, Wuhan 430081, China; Key Laboratory for Ferrous Metallurgy and Resources Utilization of Ministry of Education, Wuhan University of Science and Technology, Wuhan 430081, China; Email: zhuhy@wust.edu.cn
***Corresponding Author: Jianli Li:** The State Key Laboratory of Refractories and Metallurgy, Wuhan University of Science and Technology, Wuhan 430081, China; Key Laboratory for Ferrous Metallurgy and Resources Utilization of Ministry of Education, Wuhan University of Science and Technology, Wuhan 430081, China; Email: jli@wust.edu.cn
Lanqing Wang, Jixuan Zhao, Yue Yu: Hubei Provincial Key Laboratory for New Processes of Ironmaking and Steelmaking, Wuhan University of Science and Technology, Wuhan 430081, China

1 Introduction

Steel pipelines are widely used in petroleum and natural gas transportation, requiring that they possess a high strength and corrosion resistance. These materials are subjected to stringent requirements regarding their alloying elements, purity, and manufacturing processing [1–3]. Most importantly, surface cracks can significantly affect their service lifetimes.

Studies on the formation mechanism of reticular cracks have mainly focused on the alloying elements and precipitations in grain boundaries. Sun *et al.* [4] reported that reticular cracks are due primarily to uneven cooling on the slab surfaces. Phase transition of austenite to ferrite appear during the continuous casting process, which is accompanied by precipitations of carbide and nitride that lead to grain boundary cracks under thermal and straightening stresses. Maehara *et al.* [5] and other researchers [6–9] found that reticular cracks generally appear on Nb and V-bearing pipeline steel surfaces, for precipitation of Nb(CN), V(CN), and Ti(CN) particles decreased the hot ductility of Nb and V-bearing steels. Kajitani *et al.* [10], Fredriksson *et al.* [11], and Xiao *et al.* [12] detected distributions of residual elements in grain boundaries via SEM. Enriched regions of Cu, As, and Sn were found in the grain boundaries, which resulted in micro-cracks on the pipeline surfaces. It is generally considered that reticular cracks are related to the alloying elements and their precipitations in grain boundaries.

To date, there has been less research on the formation mechanism of reticular cracks due to metallurgical factors. Chen *et al.* [13] found inclusions containing Ca, Mg, Al, Na, and K near reticular crack zones, which were due to the fluxes from the molds in continuous casting. In our previous study, we discussed the relationship between the inner fold defects on pipeline surfaces and the associated metallurgical properties [14]. It is therefore speculated that there exists a relationship between reticular cracks and metallurgical factors.

This study considers the microscopic morphologies of reticular cracks on Nb-bearing pipeline surfaces as observed using optical microscopy. Oxidized round spots

Table 1: Chemical composition of Nb-bearing pipeline steel (wt. %).

Element	C	Si	Mn	P	S	Cu	Ni	Cr	Mo	Ti	Nb
Content	0.09	0.35	1.38	0.01	0.007	0.053	0.306	0.18	0.28	0.01	0.02

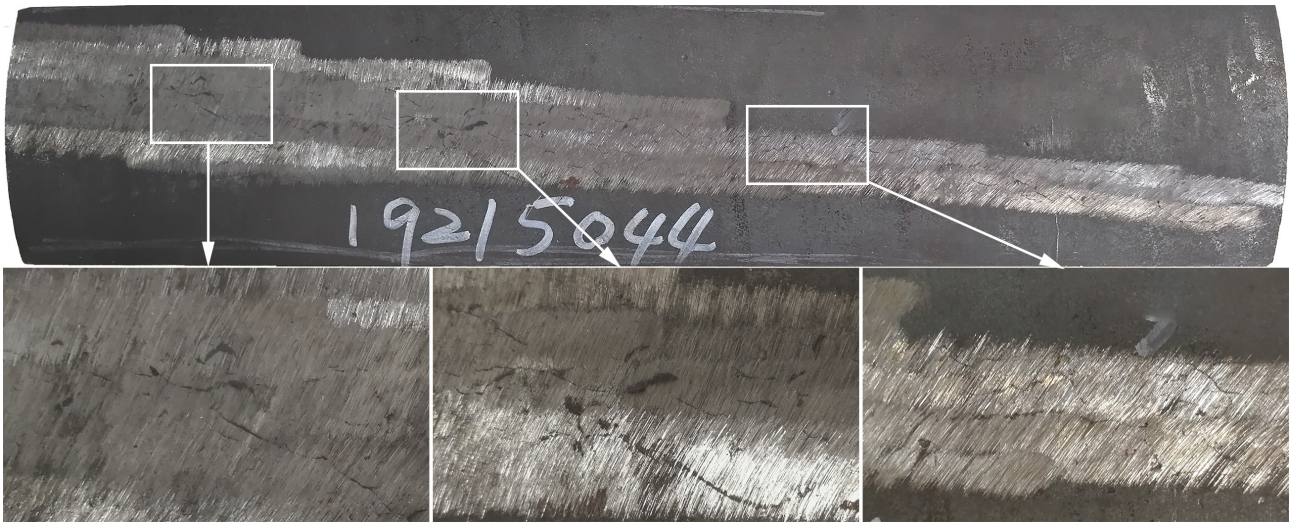

Figure 1: Typical morphology of reticular cracks on the surface of an Nb-bearing pipeline.

and the metallographic structures near such defects are detected using scanning electron microscopy (SEM). The formation mechanism of reticular cracks is discussed, and the relationship between the surface quality and the metallurgical factors for Nb-bearing pipeline steel is considered.

2 Materials and Experimental Procedure

The chemical composition of Nb-bearing pipeline steel is shown in Table 1. The fabrication process of the investigated pipeline includes the following steps: arc furnace smelting (EAF) → ladle furnace refining (LF) → vacuum refining (VD) → continuous casting (CC) → piercing → continuous rolling → sizing or sinking processes. The hot working technology for Nb-bearing pipeline steel is to heat at 1200°C for 2.5 h, while the hot rolling and finish rolling temperatures are at 1100 and 870°C, respectively.

The selected pipe section with reticular cracks was cut along its longitudinal direction. Based on the defect positions, samples of dimensions 20 mm × 20 mm were cut with a wire cutting machine. The samples were cleaned in acetone under ultrasonication to remove any oil stains from the surfaces. The microscopic morphologies of the reticular cracks and qualitative analyses of the oxidized round spots and elemental distributions near the defects were determined using a scanning electron microscope (Zeiss ASIN EVO10, Carl Zeiss Microscopy Ltd., Germany). The specimens for microstructural observations were prepared via mechanical polishing and chemical etching in a 4% nital solution and were observed using an optical microscope (Zeiss Axioplan 2 Imaging, Carl Zeiss Microscopy Ltd., Germany).

3 Results

Figure 1 shows the typical reticular cracks on an Nb-bearing pipeline surface. It can been seen that a great deal of cracks is distributed along the rolling direction. SEM was used to observe the widths and depths of microstructures from reticular cracks on radial and circumferential sections after polishing. Figure 2 shows a typical example of the microscopic morphology for a reticular crack. The crack extends from the outer surface of the steel pipe inwards at a depth of 0.24 mm and is filled with FeO. The reticular cracks are discontinuously distributed along the radial direction. It is seen from the cross-section and end profile views of the crack that it experienced a certain radial deformation during the rolling process. Thus, it is presumed that the reticular crack was formed before the rolling process.

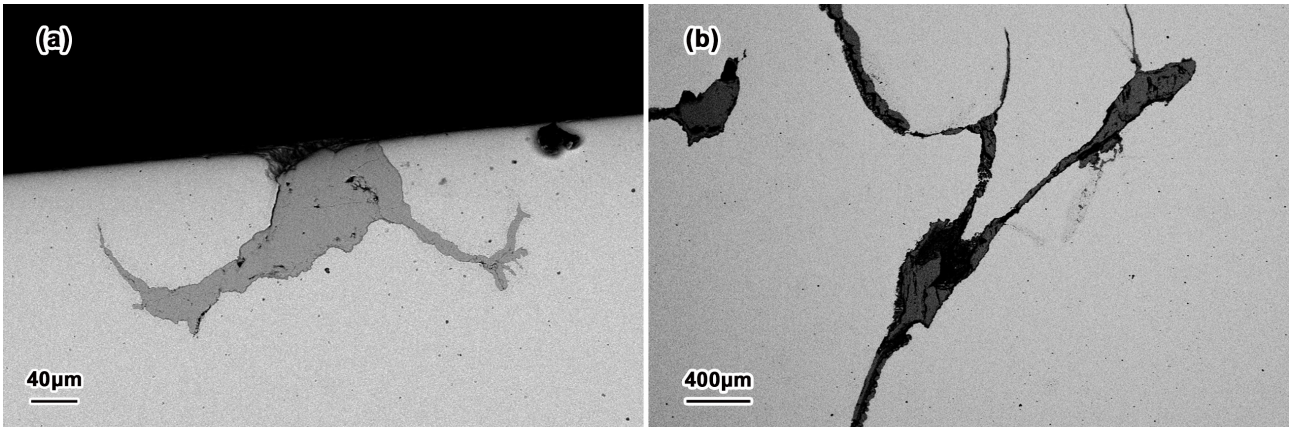

Figure 2: Cross-sectional (a) and polished surface (b) morphology of a reticular crack.

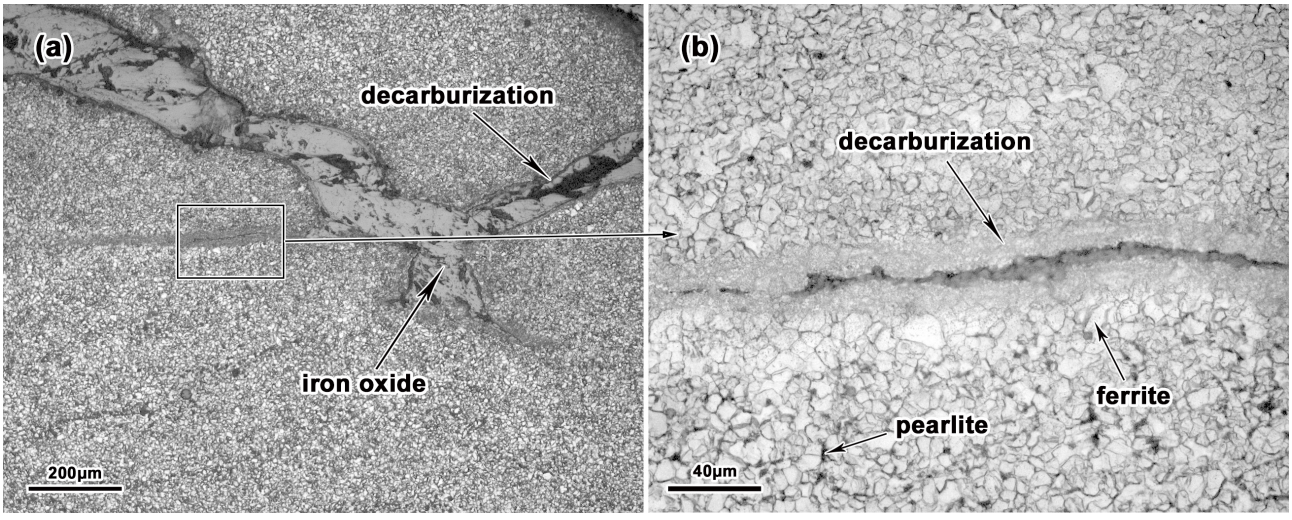

Figure 3: Metallographic structure near the reticular crack at (a) 100× and (b) 500× magnifications.

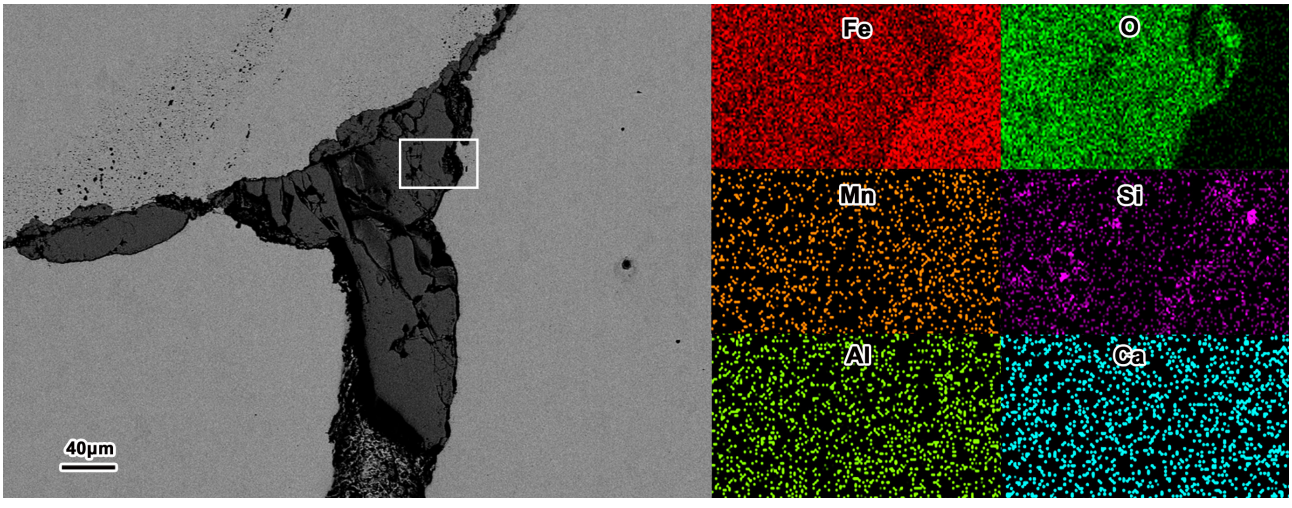

Figure 4: Element mapping of typical reticular crack zone.

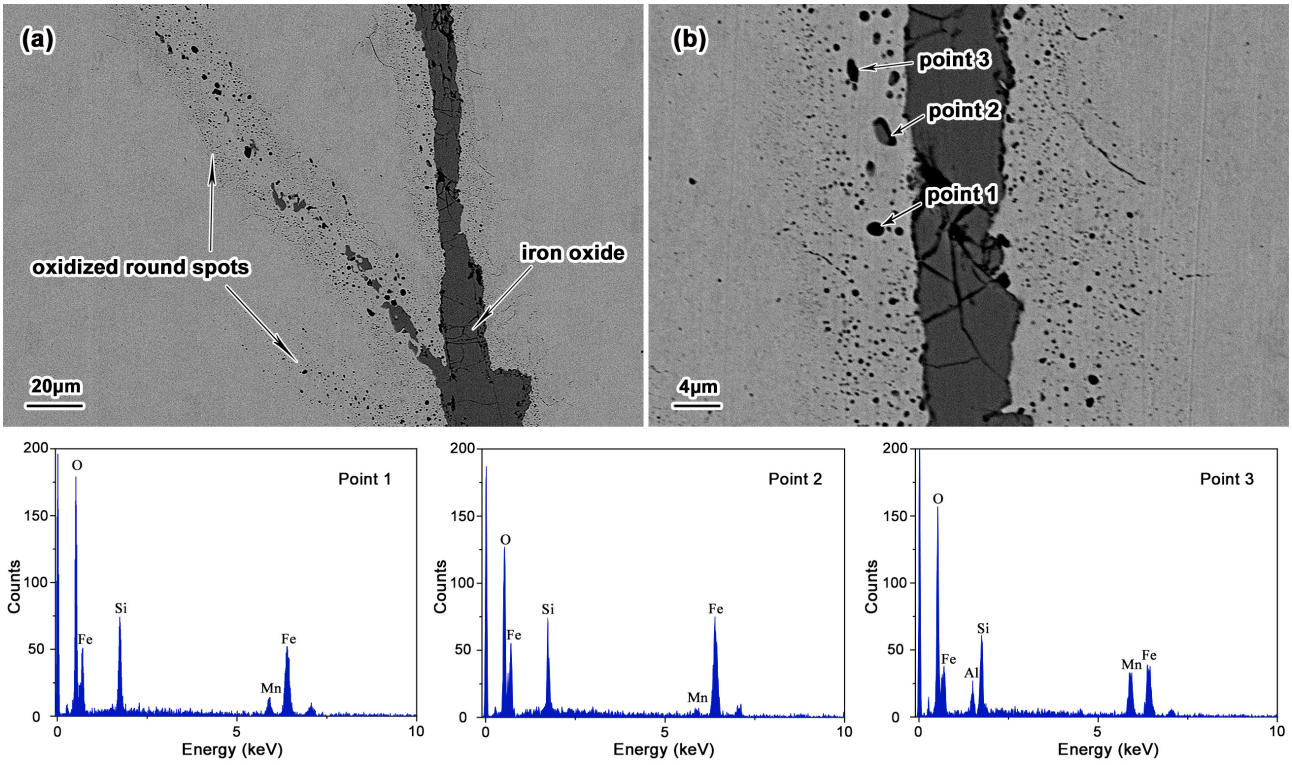

Figure 5: Microscopic morphology (a) and energy spectrum analysis (b) of the oxidized round spots in the reticular crack zone.

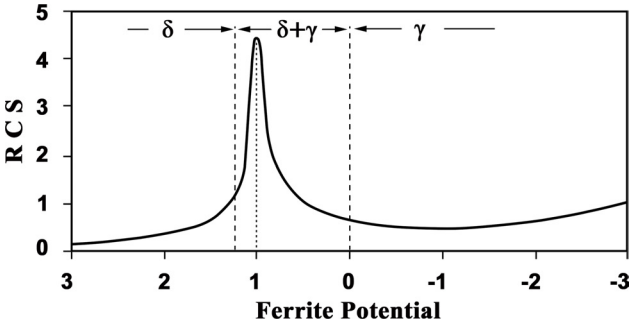

Figure 6: Relationship between the relative crack susceptibility (RCS) and ferrite potential (FP).

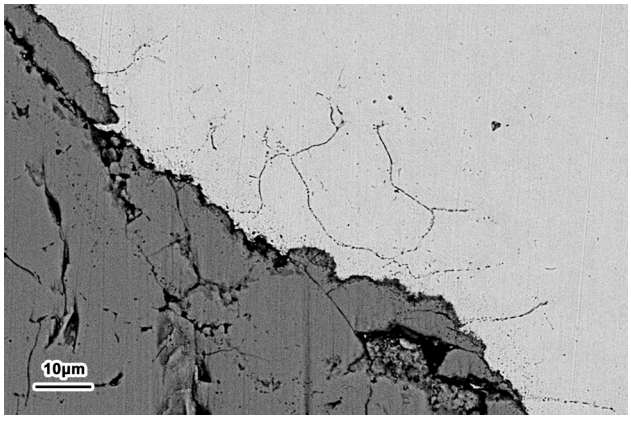

Figure 7: Microscopic morphology of the microcracks along the grain boundary.

The metallographic structure near the crack was observed after etching with a 4% nital solution. As shown in Figure 3, the metallographic structure is ferrite (black) and pearlite (white). The grain size of the ferrite near the crack region is larger, while it is smaller in the steel matrix. The crack is filled with iron oxide and there are obvious decarburization layers on both its sides that are approximately 15μm thick. It is inferred that the reticular cracks form before the heat treatment, and that their inner wall oxidized during the heat treatment to form the large amount of observed iron oxide. A decarburization layer appeared on the inner wall of the crack, which grew over time.

The end of the reticular crack was characterized using both SEM and energy dispersion spectroscopy (EDS), as shown in Figure 4 and Figure 5. Figure 4 and Figure 5a shows that the crack end is filled with a significant amount of iron oxide, and there is a large number of oxidized round spots on both sides of the crack ends. The maximum oxidized spot diameter is up to 3 μm. The spots near the crack side are larger and more intensive, while those in the steel matrix are smaller and more dispersed. Figure 5b shows the chemical composition of the oxidized round spots as

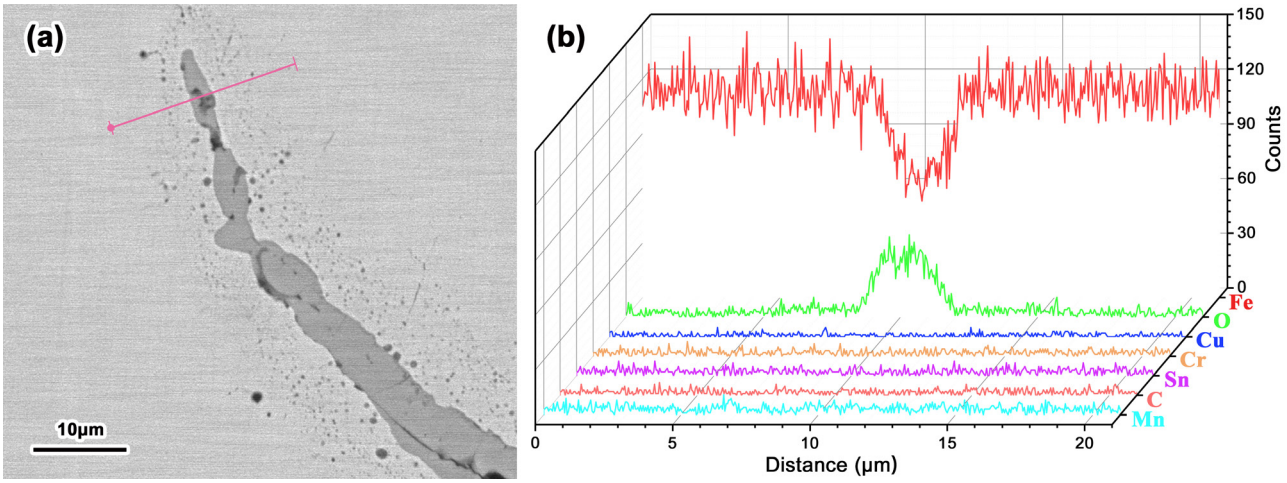

Figure 8: Line scanning analysis over the line shown in (a) for (b) Fe, O, Cu, Cr, Sn, C, and Mn.

determined using EDS. Points 1, 2, and 3 show the presence of Fe, Mn, and Si oxides, while point 3 also shows the existence of aluminum, which was used as a deoxidizing agent in the ladle furnace refining process.

4 Discussion

Two conditions need to be satisfied to form a decarburization layer and oxidized round spots. First, there has to be a relatively long oxidizing time. Second, the temperature of the heat treatment should be sufficiently high. The formation mechanism of the decarburization layer and oxidized round spots is as follows. The reticular crack is exposed to air, the heating or holding temperature is above 1000°C, and the temperature is maintained for 30 min. Then, C atoms diffuse outwards from the matrix to around the crack zone and oxidize with O atoms in the air to form CO or CO_2 gas, which then leave the slab at elevated temperatures. This causes the decarburization layer to form on both sides of the crack. In addition, O atoms diffuse from the air and into the steel matrix, which can then react with the strong oxidizing elements, such as, Si and Mn. This forms the oxidized round spots, which consist of silicon oxide, manganese oxide, or (Fe, Mn) $O{\cdot}SiO_2$ particles.

It is concluded that the reticular cracks cannot be formed during the rolling process based on the hot working production conditions mentioned in experimental procedure section, the observed decarburization near the reticular crack zone, and the distribution of oxidized round spots. The cracks formed during the rolling process have less iron oxide and no decarburization or oxidation spots in the crack zone. Thus, the reticular cracks observed in this study may have been generated during the continuous casting solidification process. The decarburization layer and oxidized round spots were then likely formed during the heating and heat preservation processes.

Pradhan *et al.* [15] assessed the effects of alloying elements on the crack susceptibility using the corresponding ferrite potential (FP) values described by Eqs. (1) and (2).

$$FP = 2.5(0.5 - \%C_P) \tag{1}$$

where

$$\%C_P = \%C + 0.02\%Mn - 0.1\%Si - 0.7\%S \tag{2}$$

The $\%C_P$ denotes the carbon equivalent, which considers the effect of the other alloying elements in the steel. Using the chemical composition of the investigated crack samples given in Table 1, The FP value for the Nb-bearing pipeline steel is found to be 1.05. The relative crack susceptibility is maximized when the FP is around 1, as shown in Figure 6 [16].

Intergranular cracks are the most predominant when the FP is around 1. The coarse grains are further embrittled because of the precipitation and enrichment of residual elements. Figure 7 shows the microscopic morphology near the crack zone, which includes intergranular microcracks. The intergranular microcracks are distributed along the primary grain boundary, while the crack boundary is decarburized. This indicates that the crack is formed before the austenite transformation at approximately 1400°C in the mold. The nascent solidified shell is formed during the solidification process with a phase transition of δ to γ. Austenite grain boundary cracking then appears due to volume shrinkage and bulging, tension, and static pressure in the molten steel. As the continuous casting process progresses, the microcracks expand to reticular cracks due

to the fabrication parameters, such as tension, bulging, misalignment, and uneven cooling.

Liu *et al.* [17] and Zhu *et al.* [18] observed the crack area of a tube bloom and slab and found that they were enriched with Cu and Cr elements near the cracks. This was mainly because the chromium coating shed from the inner wall of the copper mold during the continuous casting process, which led to a direct contact between the inner wall of the mold and tube bloom. The melting point of Cu is 1085°C, which can penetrate into the austenite grain boundary through the iron oxide skin. This reduces the grain boundary bonding force, induces intergranular cracks, and results in the formation of reticular crack. For the considered reticular crack samples, the distributions of elements, such as Cu, Cr, and Sn, near the reticular crack zone were detected using the line scanning analysis shown in Figure 8. The results indicate that the fillers in the reticular crack are Fe and O elements, and there are no obvious enrichments of Cu, Cr, or Sn within the scanning range. It is speculated that the copper mold worked as intended and that the chromium coating did not peel off. Therefore, the influence of residual elements on the reticular cracks is ruled out.

5 Conclusions

The oxidized round spots and metallographic structures near reticular cracks were investigated and their formation was discussed. The main results of this study are summarized as follows.

(1) Reticular cracks are discontinuously distributed and filled with iron oxide. Both a decarburization layer and oxidized round spots are detected on either side of the reticular crack, and the oxidized round spots near the crack sides are larger and more intense with primary chemical compositions of Fe, Mn, and Si oxides.
(2) The formation of reticular cracks occurs prior to decarburization and oxidized round spots due to the diffusion of oxygen atoms from the crack edge to the steel matrix. Reticular cracks are generated during the continuous casting solidification process, while decarburization and oxidized round spots are formed during the heating and heat preservation processes.
(3) The ferrite potential (FP) value of the considered pipeline steel is 1.05, which leads to a higher relative crack susceptibility. Intergranular microcracks are distributed along the grain boundaries, which expand into reticular cracks under due to the continuous casting parameters.

Acknowledgement: This work was supported by the National Natural Science Foundation of China (Grant Nos. 51604198 and 51874214).

References

[1] Shanmugam, S., N. K. Ramisetti, R. D. K. Misra, J. Hartmann, and S. G. Jansto. Microstructure and high strength–toughness combination of a new 700MPa Nb-microalloyed pipeline steel. Materials Science and Engineering A, Vol. 478, No. 1-2, 2008, pp. 26–37.
[2] Liu, Z. Y., X. G. Li, C. W. Du, L. Lu, Y. R. Zhang, and Y. F. Cheng. Effect of inclusions on initiation of stress corrosion cracks in X70 pipeline steel in an acidic soil environment. Corrosion Science, Vol. 51, No. 4, 2009, pp. 895–900.
[3] Zakaria, M. Y. B., and T. J. Davies. Formation and analysis of stack cracks in a pipeline steel. Journal of Materials Science, Vol. 28, No. 12, 1993, pp. 3322–3358.
[4] Sun, Y. H., C. L. Zhao, K. K. Cai, S. B. Yang, Y. Chen, G. J. Li, et al. Research of causes of surface network cracks on continuous casting slabs. China Metall., Vol. 18, 2008, pp. 15–20.
[5] Maehara, Y., K. Nakai, K. Yasumoto, and T. Mishima. Hot Cracking of Low Alloy Steels in Simulated Continuous Casting-Direct Rolling Process. Transactions of the Iron and Steel Institute of Japan, Vol. 28, No. 12, 1988, pp. 1021–1027.
[6] Billany, T. J. H., A. S. Normanton, K. C. Mills, and P. Grieveson. Surface cracking in continuously cast products. Ironmaking & Steelmaking, Vol. 18, 1991, pp. 403–410.
[7] Yasumoto, K., Y. Maehara, S. Ura, S. Ura, and Y. Ohmori. Effects of sulphur on hot ductility of low-carbon steel austenite. Materials Science and Technology, Vol. 1, No. 2, 1985, pp. 111–116.
[8] Mintz, B. Influence of nitrogen on hot ductility of steels and its relationship to problem of transverse cracking. Ironmaking & Steelmaking, Vol. 27, No. 5, 2000, pp. 343–347.
[9] Ouchi, C., and K. Matsumoto. Hot ductility in Nb-bearing high-strength low-alloy steels. Transactions of the Iron and Steel Institute of Japan, Vol. 22, No. 3, 1982, pp. 181–189.
[10] Kajitani, T., M. Wakoh, N. Tokumitsu, S. Ogibayashi, and S. Mizoguchi. Transactions of the Iron and Steel Institute of Japan, Vol. 81, 1995, pp. 29–34.
[11] Fredriksson, H., K. Hansson, and A. Olsson. On the mechanism of liquid copper penetration into iron grain boundaries. Scandinavian Journal of Metallurgy, Vol. 30, No. 1, 2001, pp. 41–50.
[12] Xiao, J. G., F. M. Wang, and H. J. Wang. Effect of residual elements Cu, As and Sn on surface micro-crack of hot rolled steel plate. Heat Treat. Met., Vol. 35, 2010, pp. 102–107.
[13] Chen, Y. Q., S. T. Qiu, G. Li, S. J. Chen, and D. W. Wang. Analysis on surface net cracks of Φ 800 mm casting bloom of steel Q345E and control measures. Spec. Steel, Vol. 39, 2018, pp. 43–46.
[14] Li, B. S., H. Y. Zhu, Z. L. Xue, Z. F. Qin, and J. Sun. Analysis of inner fold and bulge defects on J55 steel for oil casing pipe. AIP Advances, Vol. 9, No. 8, 2019, p. 085109.

[15] Pradhan, N., N. Banerjee, B. B. Reddy, S. K. Sahay, C. S. Viswanathan, P. K. Bhor, et al. Control of transverse cracking in special quality slabs. Ironmaking & Steelmaking, Vol. 28, No. 4, 2001, pp. 305–311.

[16] Wolf, M. M. Estimation method of crack susceptibility for new steel grades. Proceedings of 1st European Conference on Continuous Casting, September 23-25, 1991, Florence, Italy, pp. 2489–2499.

[17] Liu, J. B., X. W. Zhang, and Q. W. Zhang. Causes and control research of round billet surface net cracks. Contin. Cast., Vol. 41, 2016, pp. 66–70.

[18] Zhu, G. S., Y. S. Wang, X. H. Wang, and W. J. Wang. Surface net cracks of continuously cast slabs. Journal of University of Science and Technology Beijing, Vol. 27, 2005, pp. 441–443.